JOURNAL OF MATERIALS SCIENCE **40** (2005) 761–766

Lateral grain growth during reactive isothermal solidification in the Ni-Sn system

D. GUR, M. BAMBERGER
Department of Materials Engineering, TECHNION, Israel Institute of Technology

In this research lateral growth of Ni_3Sn_4 grains in the Ni-Sn system during isothermal solidification was investigated. Experiments involved multi-layered samples heat-treated for different durations at temperatures in the range 235–600°C. During solidification Ni_3Sn_4 was the only intermediate phase found to grow as a layer at the solid/liquid interface. SEM and optical microscopy cross-sectional views of samples heat-treated at 500°C and at 600°C reveal that lateral grain growth occurs, the mean lateral grain size being proportional to $\sqrt{t}$(t-the duration of the heat treatment). This process was found to be connected with solution reprecipitation process between adjacent grains in order to equate the local curvature of the solid/liquid interface at groove zone. Rotation of the grain boundary groove due to this mass transfer induces a curvature of the grain boundary, which is the controlling mechanism for its migration. The process was numerically formulated, which provides quantitative fitting to the observed kinetics. The formulation includes a contribution due to the good wetting of the grain boundaries by the liquid phase supporting the observed enhancement in growth rate.

1. Introduction

In a binary system Reactive Isothermal Solidification involves the formation of intermetallic compounds at the solid/liquid interface. The process can be regarded as one of diffusion in a solid-liquid couple, but deviations from the classical behavior have been observed [1–6].

During the solidification of the Ni-Sn system, in the temperature range, 235–600°C, only the Ni_3Sn_4 intermediate phase was found to grow. In experiments on multi-layered model specimens this phase grows into the liquid as a coarse-grained layer, one grain in thickness [6]. Simultaneously with its growth a lateral grain growth occur within the layer plane. The process resembles the mechanism of grain growth and coalescence during liquid phase sintering [7–11].

In the present work it was found that the lateral growth of the Ni_3Sn_4 layer grains is more rapid during the presence of the liquid phase in the system than in cases where all the liquid phase was consumed before the experiment was finished.

A mechanism to describe this accelerated lateral growth of Ni_3Sn_4 grains is proposed which is based on normal grain growth model and involves a contribution due to the good wetting by the liquid phase.

2. Experimental procedure

The experiments were performed on multi-layered samples made of alternating sequences of Ni/Sn pairs of foils, of a thickness, in microns, of: 150/100, 150/10, and 6/10. These sequences were embedded in Ni powder and die-pressed to form $18 \times 18 \times 5$ mm^3 compact samples in a procedure for cold sintering under high pressure [12]. The Ni powder envelope served to fix the multi-layer structure during melting occur and to act as a protective shield against oxidation during heat treatments. The Ni foils used were 150 μm BDH 99.9 wt.% pure and 6 μm ALFA 99.95 wt.% pure; the Sn foils: 100 μm BDH 99.5 wt.% pure and 10 μm Reidel-deHaen 99.9 wt% pure.

The samples were heat-treated for different duration at temperatures in the range, 235–600°C. Phase growth kinetics are described elsewhere [6]. In the present work the grain growth process was examined mainly at 500°C and 600°C, while the focus will be on experiments at 500°C. At the above given temperature range the Sn layers were in the liquid state. After the treatment the samples were water-quenched to room temperature.

The grain size measurements were performed on metallographic cross sections of the multi-layered samples. The mean lateral grain size given in Fig. 3 is an average of about 10–20 grains. Phase characterization was obtained by X-Ray diffraction in a Bragg-Brentano—Philips PW-1820 diffractometer equipped with the PW-1700 APD package on a micro VAX computer. Cu tube and Graphite monochromator provided Cu K_α radiation. The microstructure was characterized with a ZEISS AXIOPHOT optical microscope and a JEOL JSM-840 scanning electron microscope. Operational voltages were 10 and 20 Kilovolts. Local composition measurements were made with an AN10000 link system which included ZAF correction. Sample preparation for X-Ray examination included polishing to the 0.3 micron degree of roughness using alumina particles as abrasive. For metallographic examination,

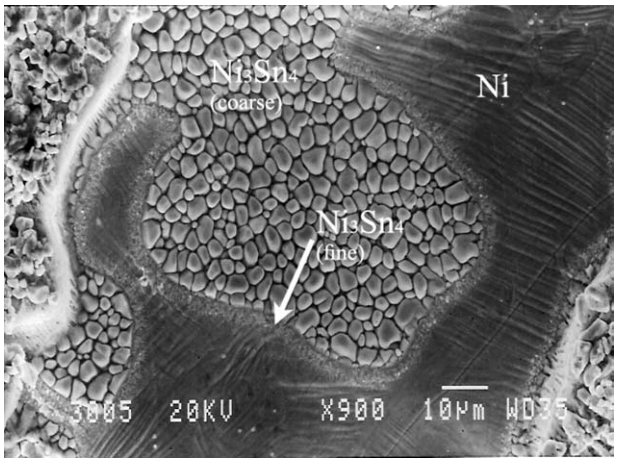

Figure 1 SEM flat-on view of a multi-layer sample heat-treated at 500°C for 30 s.

polishing as above was followed by etching in a solution of 5 gr. $FeCl_3$, 2 ml. HNO_3, and 98 ml ethyl alcohol.

3. Results

Fig. 1 shows a flat-on view of a multi-layered sample heat-treated at 500°C for 30 s. This SEM micrograph was obtained by peeling the layers of the specimen. The Ni_3Sn_4 island is surrounded by a layer of fine grains of the same phase and bordering the unreacted Ni foil. The size distribution of the Ni_3Sn_4 grains and the faceted morphology of the grains can be observed. In the cross-sectional view (Fig. 2) of a typical sample, which was heat treated at 500°C for 5 min, the grains exhibit a smooth curvature at the interface with the liquid Sn(Ni). Deep grooves are found at grain boundaries. On counting the lateral size of the grains (taken as the distance between the two grain boundary grooves of a grain) on several cross-sectional micrographs of specimens heat-treated at 500°C and 600°C , for different durations, it was found that the mean lateral grain size depends linearly on $\sqrt{t}$. This is shown by the diamond and the triangle marks for 500°C and 600°C respectively, in Fig. 3. The two square marks refer to the lateral size of grains in a thinner layer, in which solidification was completed before the end of the heat treatments at 500°C, indicating a slower growth rate when the liquid phase is no longer present.

Fig. 4 is an optical micrograph of a sample heat-treated at 500°C for 120 min. This micrograph was taken with a polarized light source which enables observations of the differences in contrast between two adjacent grains and their grain boundaries.

From these micrographs the following can be concluded: (1) In case of two adjacent grains of similar lateral sizes the direction of the groove is perpendicular to the layer, whereas when a large grain is in contact with a smaller one, the groove is inclined towards the small grain; (2) In this latter case, the grain boundary curvature in the cross-sectional view (which is more significant than the curvature observed in flat-on view) corresponds to the groove rotation towards the smaller grain; (3) In some of the large grains there are zones of negative curvature at the interface with the liquid. Based on these observations the following mechanism of the lateral grain growth of the Ni_3Sn_4 phase during Isothermal Solidification is proposed.

4. Discussion

At the beginning of solidification, the Ni_3Sn_4 intermediate phase nucleates at the interfaces between the pure Ni and Sn layers. It is assumed that after a while Ni_3Sn_4 grains are randomly distributed at the interface. Diffusion processes through the liquid phase cause that layer to grow rapidly. In the prevailing high-temperature regime (500°C, 600°C) lateral growth of the grains, which have smooth interfaces (as in Fig. 2) with the liquid, takes place. This is radically different from the faceted morphology that exists at lower temperatures [6,13,14].

Figs 1 and 2 show that the significant curvature is the one observed in the cross-sectional view, as against the curvature between similar grains in the flat-on view. In Fig. 2, a groove and a small angle between two adjacent grains can be seen at point A. The radius of curvature of the liquid/solid interface of the small grain, to the right of point A differs from that of the larger grain, to the left of A. Therefore, there will be diffusion from the smaller grain to the bigger one, resulting in coalescence of these grains. This is evident at point B, where a grain boundary between the grains can't be discern

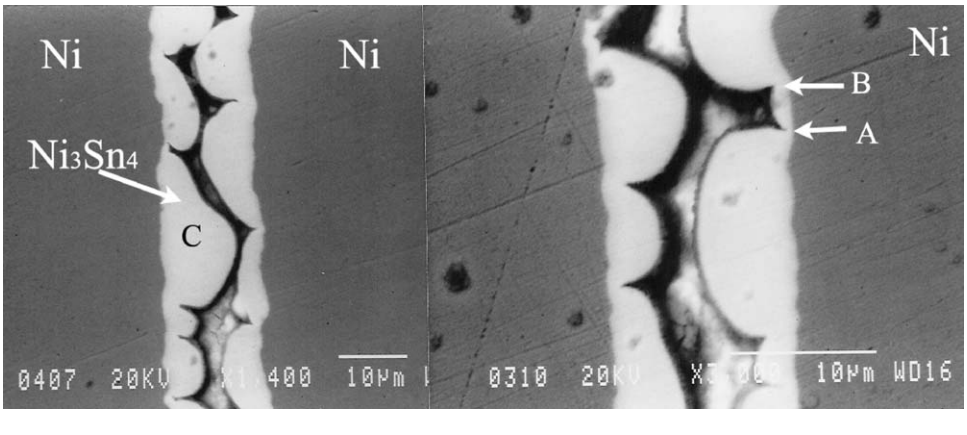

Figure 2 Cross-sectional SEM micrograph of a sample heat-treated at 500°C for 5 min.

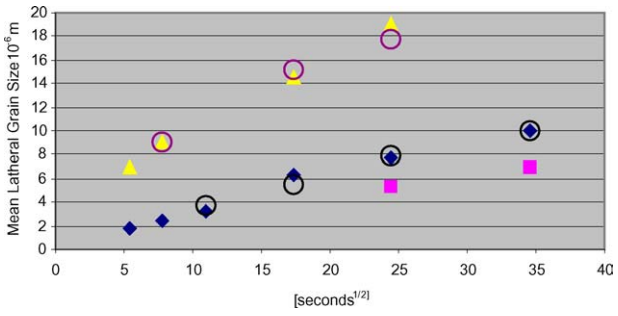

Figure 3 Experimental results: Mean lateral size of Ni_3Sn_4 grains as a function of time at 500°C (diamond marks), and at 600°C (triangles). The square marks represent the growth process, which took place partly after solidification was completed (at 500°C). Simulation: Calculated growth kinetics at 500°C (Circles).

and the angle between them is bigger than that at point A. Assuming that the grain located between A and B was symmetric around its tip, it can be concluded that at point B the adjacent grains merged into one, while the previous grain-boundary rotated to form a more stable surface. A more advanced situation can be seen at point C in Fig. 2. The negative radius of curvature at point C cannot be formed during grain growth into the liquid and hence the large "grain" seen there is in fact two grains in a transition towards being one big grain by coalescence. During this process the newly formed grain is no more symmetric, but the difference in the interfacial energy between the positive and negative radii of curvature will finally result in a symmetric grain. It may be concluded that the coalescence is connected with grain's rotation [15] and diffusion controlled solid-state migration of the grain boundaries, in which the two grains become one [14]. The grain growth mechanism will be presented as consequential stages in the following.

A schematic description of the Ni_3Sn_4 layer is shown in cross-sectional view in Fig. 5a. The two adjacent grains are of different lateral sizes, and are separated by a groove at the boundary. The corresponding three surface tension vectors are presented on the assumption that local thermodynamic equilibrium exists at the triple point, which dictates a constant dihedral angle ϕ.

The concentration of the liquid phase at the solid-liquid interface depends on the curvature of the Ni_3Sn_4 grains in accord with the Gibbs-Thomson equation. Therefore, at groove zone when a large grain with a low curvature is adjacent to a small grain with a high curvature, a gradient in the chemical potential exists as the driving force for mass flow in the liquid between the two grains. Thus, mass transfer through the liquid phase or a solid-state dissolution process takes place between the adjacent grains, as discussed for the case of two grains which are in contact during liquid phase sintering [10, 14]. This mass transfer occurs also between the groove zone and the flat surface in grain boundary grooving by bulk diffusion [16, 17].

The curvature-induced mass transfer process between the grains stops when the local curvatures of the two grains at groove zone are equal, i.e. material will transfer from the small grain to the large one, resulting in a rotation of the grain boundary groove towards the small grain (Fig. 5b). The equal local curvatures obtained at groove zone of two grains, which are in contact during liquid phase sintering, can be clearly observed in the figures of Kim and Yoon [11].

In the present situation, however, this rotation due to the local solid-state dissolution process occurs simultaneously with the phase growth process in which Ni, supplied from the grain boundary groove reacts with Sn at the solid-liquid interface of the grains, to form the Ni_3Sn_4 phase. Due to groove rotation a curved grain boundary will be obtained in order to preserve the local thermodynamical equilibrium at the triple point (Fig. 5b).

The following formulation describes the situation of a cylindrical grain boundary with a curvature of $1/r$.

If θ is the angle of rotation of the three surface tension vectors, the grain boundary curvature, K_{gb}, can be expressed as:

$$K_{gb} = 2\mathrm{Sin}\theta / L \tag{1}$$

where L is the grain boundary depth (layer thickness at the grain boundary, as in Fig. 5a). In the following the assumption is that the boundary is perpendicular to the plane of the paper. Genin *et al.* [18] discussed a similar mechanism for the rotation of thermal grooves between grains in thin homogeneous metal layers for which mass transfer was carried out by surface diffusion. They predicted that this rotation, which contributes to the grain boundary curvature, can cause a grain growth process in the layer. Similar mechanism was discussed by Kim and Yoon [11] for the migration of grain boundary between a large and a small grain which are in contact during liquid phase sintering.

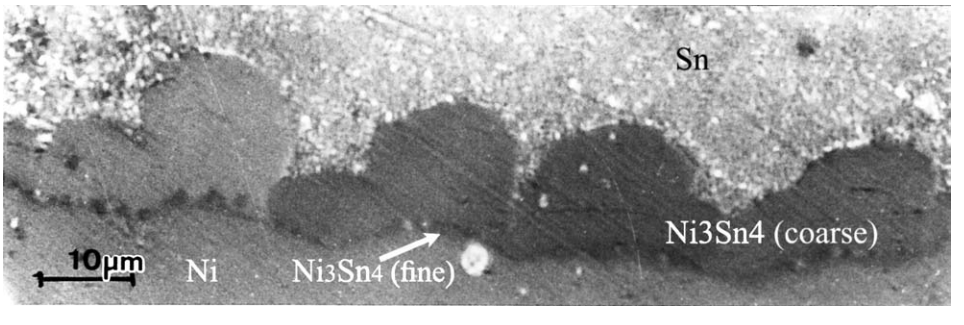

Figure 4 Optical micrograph in cross-sectional view and under polarized light, of a sample made of 150/100 μm thick Ni/Sn pairs of foils heat-treated at 500°C for 120 min.

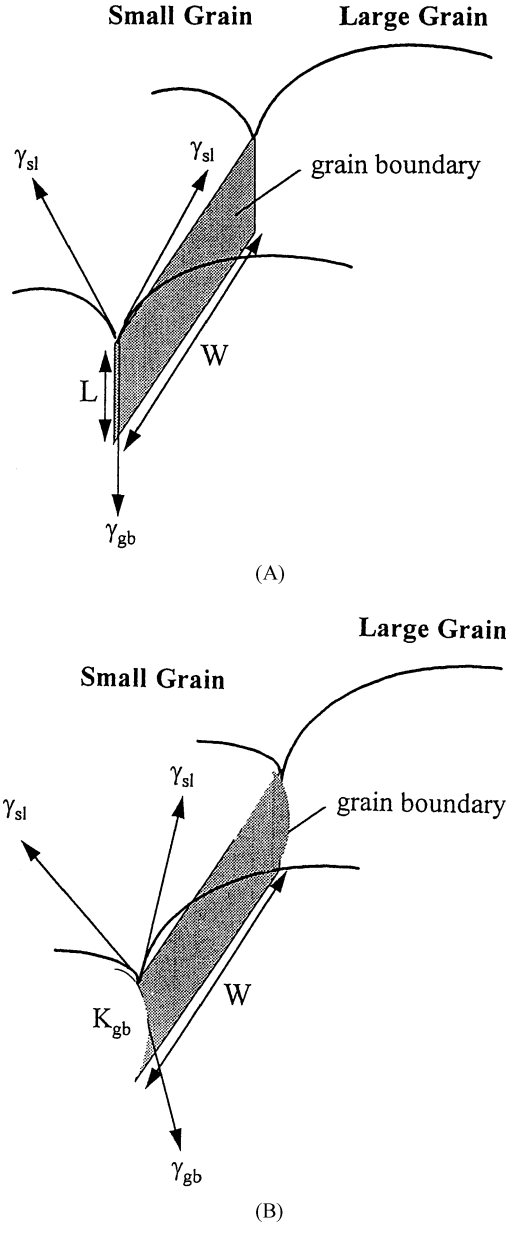

Figure 5 Schematic illustration of the lateral growth process.

According to Genin *et al.* [18], for grains of two sizes D_1 and D_2 the surface of which are at equilibrium, i.e. their curvatures are equal (see Fig. 6), the corresponding angle of rotation of the grain boundary is:

$$\mathrm{Sin}\theta = Q(D_1 - D_2)/(D_1 + D_2) \qquad (2)$$

$Q = \gamma_{gb}/2\gamma_{sl}$
γ_{gb}: grain boundary surface energy,
γ_{sl}: solid/liquid interficial energy.

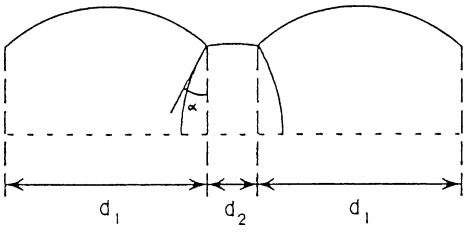

Figure 6 One-dimensional array of grains with constant curvature at their boundaries [9].

The surface energies are assumed to be independent of the orientation.

This expression, which takes into account the curvatures of the adjacent grains (through their sizes) and the wetting conditions, was adopted for the formulation of the lateral grain growth process. The lateral grain growth in Ni_3Sn_4 that was found in this work is similar to the grain growth by grain boundary migration during liquid phase sintering. However, there are several differences between them.

1. Simultaneously with the lateral grain growth in the coarse grained Ni_3Sn_4layer its overall volume increases. In addition, fine grained Ni_3Sn_4 layer grows at the interface with the solid [6].

2. In the present case all layer grains forms boundaries with each other (non-zero dihedral angle is obtained). The grains grow as a flat layer and the measured quantity was the lateral size (distance between grain boundary grooves). In liquid phase sintering the majority of the grains, and major grain surface as well, are surrounded by liquid. Therefore the Ostwald ripening process and the $t^{1/3}$ kinetics for coalescence [14, 19, 20] control the overall grain growth. One can find the lateral grain growth similar to two dimensional normal grain growth process in a thin solid layer which is enhanced due to the presence of the liquid phase (in the third dimension).

3. The asymmetrical conditions for the local thermodynamical equilibrium of the triple point at the two sides of the layer. The other triple point is at the interface between the coarse and the (solid) fine Ni_3Sn_4 layers.

4. Unlike the models of coalescence by grain boundary migration in sintering the grain boundary depth - L is not a simple function of grain diameter and dihedral angle, like the neck diameter - y in Kim and Yoon's work. This is due to the fact that the grain boundary grooves act as the Ni source for phase growth. Therefore, different conditions of dissolution process and diffusion fields exists there.

5. In the two-grain coalescence model by solution-reprecipitation and grain boundary migration proposed by Kim and Yoon [11] the small grain (assumed smaller than the average) is surrounded by liquid. Thus simultaneously with boundary migration, dissolution of the entire grain surface occurs, which further increases the grain boundary curvature and ,hence, the driving force for migration increases. This is not the case in the lateral grain growth process, in which as long as the boundary is not migrating, the curvature of the small grain is decreasing due to the rotation of the groove. In the present situation the grain boundary velocity is expected to change in a different manner.

The observed kinetics supports the assumption that the curvature induced grain boundary migration is the controlling mechanism (similar to a normal grain growth process) and that the processes connected with the liquid phase are fast enough, thus not providing a major contribution to the kinetics. Therefore, the following expressions will be suggested for the lateral grain growth process.

The grain boundary velocity (in the direction normal to the boundary), V_{gb}, can be described by [21, 22]:

$$V_{gb} = d(D_i)/dt = M_{gb}\gamma_{gb}K_{gb} \quad (3)$$

in which
M_{gb}: grain boundary mobility;
γ_{gb}: grain boundary energy;
K_{gb}: grain boundary curvature.

In order to simplify the mathematical formulation of the grain growth process, the total volume of material is assumed to be conserved. The phase growth, which occurs simultaneously can decrease the migration rate as discussed by Kim and Yoon [11] in the case of reprecipitation on both grains in contact. In the 500°C and 600°C heat treatments the growth of the Ni_3Sn_4 phase is assumed to be slow enough in comparison with the lateral grain boundary migration, having minor influence on it. The fast grain growth and the relatively high lateral size in comparison to layer thickness, is in agreement with this assumption. This is not the case for heat treatments at lower temperatures (350°C and below) in which, due to low grain boundary mobility, migration rate is lower in comparison to layer growth into the liquid. This results in an elongated morphology of the layer grains towards the liquid, following a further suppression of the lateral grain growth process and finally leads to crumbling of the grains into the liquid due to a dissolution process which takes place at the Microstructural-Transition-Zone [6].

The cross-sectional area, A, swept by the boundary during its migration is:

$$A = L \bullet W \quad (4)$$

in which W is the dimension perpendicular to L and to the plane of the paper in Fig. 5. When trying to approximate W it can be observed in a soap bubble model that, if $D_1 = D_2$, then $W \cong D/2$ and that if $D_1 \gg D_2$, then $W \cong D_2$, as shown in Fig. 7.

A useful interpolation formula covering these two limit cases reads

$$1/W_{1,2} = 1/D_1 + 1/D_2 \quad (5)$$

This expression for W was proposed in order to describe the grain boundary dimension parallel to the Ni_3Sn_4 layer plane (flat-on view). From this point of view grain boundary morphology is like in a thin solid layer. The expression for W is in good agreement with Equation 3 in Kim and Yoon work [11] describing the neck (grain boundary) diameter (substituting the limiting radii: $r_1 \gg r_2$ and $r_1 = r_2$). Combining Equations 1–5 and using conservation of volume, yields for the growth rate:

$$\left(\frac{\pi}{2}\right) D_i^2 \frac{d(D_i)}{dt} = -\left(\frac{\pi}{2}\right) D_{i+1}^2 \frac{d(D_{i+1})}{dt} = K \cdot D_i \left[\frac{\frac{D_i}{D_{i+1}} - 1}{\left(\frac{D_i}{D_{i+1}} + 1\right)^2}\right] \quad (6)$$

where the growth constant $K = M_{gb}\gamma_{gb}^2/\gamma_{sl}$

Equation 6 can be solved numerically for a given initial grain size distribution.

The model calculates at each time step the size of one- or two-dimensional adjacent grains, which were initially randomly distributed. Then a new mean diameter is calculated.

Computer simulation of this growth process by using Equation 6 for a one-dimensional distribution of 50 grains taken from the flat-on view (Fig. 1), fits fairly the parabolic kinetics of the lateral grain growth presented by the open circles in Fig. 3 and the value reported for the growth of Ni_3Sn_4 intermetallic layer in Ni/Sn diffusion couple in the solid state [23].

This formulation of the lateral growth process assumes that all the processes that take place in the liquid phase are very fast and do not control the growth; they were therefore not included in the model. From the simulation, growth constants K, of roughly, 1.3 μ^2/s and 5.5 μ^2/s were obtained for 500°C and 600°C respectively. These values are quite common and fall within the range of grain boundary mobility in other systems [24, 25]. Activation energy of about 81 KJ/mole was calculated for this solid-state diffusion-controlled growth process. This value falls within the range of activation energies for grain growth in metals [23, 25, 26].

One parameter, which is connected to the liquid phase, is the solid/liquid interfacial energy. When examining the equation for the growth, the deviation from the usual (solid state) growth constant, $M_{gb}\gamma_{gb}$, is the multiplier γ_{gb}/γ_{sl}, which is in fact $2\cos(\phi/2)$. From measurements of the dihedral angles (at 500°C) an average of about 30° was obtained indicating good wetting conditions. The corresponding γ_{gb}/γ_{sl} ratio of 1.93 contributes to the increase in growth rate compared with the solid-state growth illustrated by square marks in Fig. 3.

High values of this ratio providing sharp grooves will allow higher groove rotation angle and hence higher grain boundary curvature and driving force for its migration. As a consequence, an increase in growth rate will be obtained.

In the work of Buist *et al.* [7], and Stephenson and White [8] the rate of grain growth during liquid phase sintering was found to be inversely proportional to the dihedral angle ϕ conforming to the proposed model.

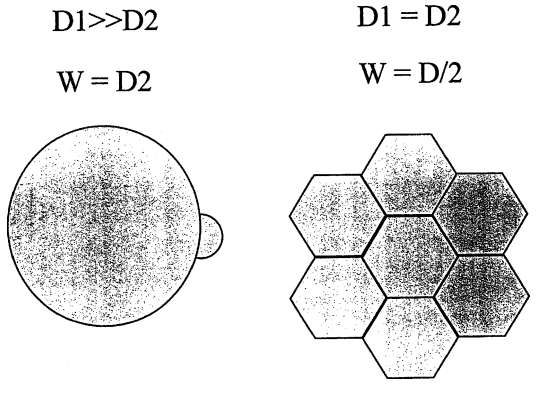

Figure 7 Two limiting values of W.

5. Conclusions

During reactive isothermal solidification in the Ni-Sn system lateral grain growth of the Ni_3Sn_4 intermediate phase was observed. The process is controlled by grain boundary migration and obeys parabolic kinetics, in which the mean lateral grain size is proportional to $\sqrt{t}$.

This process involves two mechanisms: (a) Mass transfer through the liquid phase, between grains of dissimilar curvature at the liquid/solid interface; (b) Consequent lateral migration of the grain boundary. The process can be formulated numerically in a manner similar to normal grain growth models. The growth constant of the process contains the factor γ_{gb}/γ_{sl} which represents the contribution of the good wetting condition between the Ni_3Sn_4 grain boundaries and the liquid and is responsible for the enhanced growth rate as compared with growth rate in the absence of the liquid phase.

References

1. J. A. VAN BEEK, S. A. STOLK and F. J. J. VAN LOO, *Z. Metallkde.* **73** (1982) 439.
2. S. BADER, W. GUST and H. HIEBER, *Acta Metall. Mater.* **43** (1) (1995).
3. V. N. YEREMENKO, YA. V. NATANZON and V. I. DYBKOV, *J. Mater. Sci.* **16** (1981) 1748.
4. C. L. TSAO and S. W. CHEN, *ibid.* **30** (1995) 5215.
5. V. I. DYBKOV, *ibid.* **21** (1986) 3078.
6. D. GUR and M. BAMBERGER, *Acta Materialia* **46** (1998) 4917.
7. D. S. BUIST, B. JACKSON, I. M. STEPHENSON, W. F. FORD and J. WHITE, *Trans. Br. Ceram. Soc.* **64** (1965) 173.
8. I. M. STEPHENSON and J. WHITE, *ibid.* **66** (1967) 443.
9. R. WARREN, *Int. J. Powder Met. Powder Tech.* **13**(4) (1977) 249.
10. SU SOK KANG and DUK N. YOON, *Metall. Trans. A* **13A** (1982) 1405.
11. SUNG SOO KIM and DUK N. YOON, *Acta Metall.* **31**(8) (1983) 1151.
12. E. Y. GUTMANAS, *Powder Metall. Inter.* **15** (1983) 129.
13. G. GHOSH, *J. Appl. Phys.* **88** (2000) 6887.
14. *Idem.*, *Acta Metall.* **48** (2000) 3719.
15. R. M. GERMAN, A. BOSE and S. S. MANI, *Metall. Trans. A* **23A** (1992) 211.
16. W. W. MULLINS, *Trans. Metall. Soc. AIME* **218** (1960) 354.
17. C. A. STEIDEL CHE-YU LI and C. W. SPENCER, *ibid.* **230** (1964) 84.
18. F. Y. GENIN, W. W. MULLINS and P. WYNBLATT, *Acta Metall. Mater.* **40**(12) (1992) 3239.
19. I. M. LIFSHITZ and V. V. SLYOZOV, *J. Phys. Chem. Solids* **19** (1961) 35.
20. C. WAGNER, *Z. Electrochem.* **65** (1961) 581.
21. G. ABBRUZZESE and K. LUCKE, *Acta Metall.* **34**(5) (1986) 905.
22. H. V. ATKINSON, *ibid.* **36**(3) (1988) 469.
23. W. J. TOMLISON and H. G. RODES, *J. Mater. Sci.* **22** (1987) 17669.
24. HSUN HU, "The Nature and Behavior of Grain Boundaries" (London Presss, 1972).
25. G. A. CHADWICK and D. A. SMITH, "Grain Boundary Structure and Properties" (Academic Press, 1976).
26. H. V. ATKINSON and D. M. DUFFY, *Acta Metall.* **34**(12) (1986) 2371.

Received 3 June 2002
and accepted 14 October 2004